IOP PUBLISHING METROLOGIA
Metrologia **45** (2008) 275–280 doi:10.1088/0026-1394/45/3/003

Thermal voltage converter calibrations using a quantum ac standard

Thomas E Lipe[1], Joseph R Kinard[1], Yi-Hua Tang[1], Samuel P Benz[2], Charles J Burroughs[2] and Paul D Dresselhaus[2]

[1] Quantum Electrical Metrology Division, National Institute of Standards and Technology, Gaithersburg, MD 20899-8171, USA[3]
[2] Quantum Electrical Metrology Division, National Institute of Standards and Technology, Boulder, CO 80305-3328, USA

Received 7 January 2008
Published 10 April 2008
Online at stacks.iop.org/Met/45/275

Abstract
We report on the first-ever use of a quantum ac source to calibrate a thermal transfer standard as part of the NIST calibration service for such devices, with reductions in calibration uncertainty of as much as an order of magnitude over traditional ac–dc transfer methods. We briefly describe the basic quantum ac calibration system, its operation and measurement results. An analysis of the uncertainties for the measurements is presented and plans for further development are described.

(Some figures in this article are in colour only in the electronic version)

1. Introduction

Historically, alternating (ac) voltage is most accurately measured by comparing the heating effect of an unknown ac signal with that of a known direct (dc) voltage using a thermal voltage converter [1, 2]. These devices employ one or more thermocouples arrayed along a heater structure to sense the heat generated by the unknown ac waveform. When compared with the thermocouple output generated by the average of both polarities of dc voltage, the ac–dc difference of the thermal converter can be determined, and this quantity can then be used to determine the root-mean-square (rms) value of an ac waveform directly in terms of a dc reference voltage. Thermal transfer standards (TTSs) used in this fashion are inherently insensitive both to relatively small harmonic distortions of the ac waveform and to slowly changing environmental conditions.

The NIST primary standards for ac voltage are a group of multijunction thermal converters (MJTCs) [3, 4]. Both simulation and measurement indicate that these devices have ac–dc differences of less than 1 μV V^{-1} at a few volts and audio frequencies. Range-to-range scaling techniques are used to determine the ac–dc differences in TTSs at voltages ranging from a few volts of the primary standards down to 2 mV. These range-to-range scaling techniques can be difficult to perform and depend on well-constructed thermal converters with small voltage coefficients. The uncertainties assigned to the thermal converters escalate rapidly with decreasing voltage, so that at 2 mV, the uncertainties are several orders of magnitude greater than at the 2 V level of the primary standards (270 μV V^{-1} at 1 kHz as compared with less than 1 μV V^{-1}). The performance of contemporary ac–dc transfer instruments at these low voltages is good enough that the large uncertainties associated with traditional scaling techniques are no longer adequate for characterizing these instruments in a calibration service for NIST customers. In addition, the philosophical argument can be made that ac quantities are not closely, if at all, referenced to SI (Système International) units, a situation that is increasingly untenable given the focus of the metrology community on fundamental constants.

To satisfy the increasingly stringent requirements of NIST calibration customers for reduced uncertainties on the millivolt ranges of TTSs, and to bring ac voltage metrology closer to SI units, we have developed and deployed an ac source based on pulse-driven programmable Josephson junction arrays. This ac Josephson voltage standard (ACJVS) has recently been used to calibrate a customer's TTS as part of a routine calibration service at NIST [5]. The uncertainties for this quantum-based calibration are, at some points, an order of magnitude smaller than the uncertainties based on traditional range-to-range scaling. This paper reports the first use of a practical method to disseminate ac voltage based on a quantum standard and represents a completely new paradigm for ac voltage metrology.

[3] Electronics and Electrical Engineering Laboratory, NIST, US Department of Commerce. Contribution of the United States Government. Not subject to copyright in the United States.

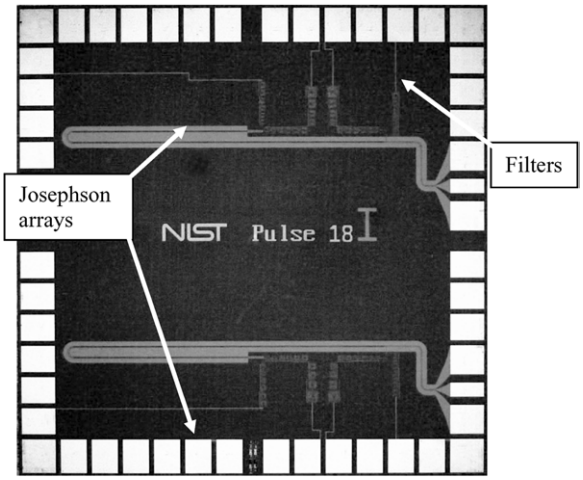

Figure 1. Photograph of a 100 mV ac Josephson chip fabricated by NIST. The chip is 1 cm square.

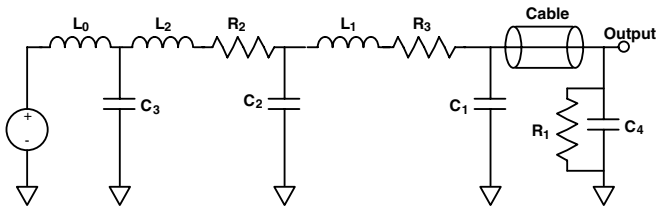

Figure 2. Simplified schematic of the output transmission line of the ACJVS.

2. ACJVS circuits

The intrinsic accuracy of the ACJVS is derived from the perfect quantization of voltage pulses generated by each Josephson junction in the array [6–9]. The ACJVS produces ac waveforms using a digital-to-analogue synthesis technique based on delta–sigma modulation and oversampling. The precise control and timing of the quantized pulses allow the synthesis of waveforms with accurate and calculable voltages. The Josephson chip contains two series arrays of Josephson junctions, each of which is independently biased and separately tuned. We have measured four different ACJVS chips, three of which had 2560 junctions in each array, providing a maximum output voltage of 100 mV with all 5120 junctions operating in series. The fourth chip features two arrays, nominally of 5120 junctions each, providing a maximum output voltage of 200 mV. Owing to memory limitations in the digital code generator, the lower limit for the output frequency is about 1 kHz, although in practice we did not use the ACJVS at frequencies below 2.5 kHz. The test article for these measurements was a commercially available, multi-range TTS of a type commonly used in ac metrology laboratories. A photograph of a typical 100 mV ACJVS chip is shown in figure 1.

3. Output transmission line

A schematic of the circuit used for these measurements is shown in figure 2. From the voltage output terminals of each Josephson array, about 1.2 m of twisted pair magnet wire conducts the voltage up the cryoprobe to the output connector. A 50 Ω coaxial lead approximately 1 m long connects the transfer standard to the ACJVS, in sequence, through a resistor, 3 MHz, 3-pole low-pass filter and a coaxial choke to the input of the transfer standard. The input impedance of the transfer standard itself decreases from 10 MΩ at dc to about 3.3 MΩ at 100 kHz. Although the amplitudes of the digitization harmonics below 10 MHz are negligible due to the oversampling ratio, the bandwidth of the TTS is sufficiently broad that the low-pass filter is required to remove the higher frequency digitization harmonics.

Table 1. Typical corrections to the measured ac–dc difference due to the transmission line. A plus sign means ac supplied to TTS is larger than the ac at the chip. The corrections are slightly level dependent due to different load terminations for the different transfer standard ranges. Corrections for 20 kHz are presented for completeness.

TTS range	Frequency	Correction/μV V^{-1}
220 mV	2.5 kHz	0
	5 kHz	+1
	10 kHz	+3
	20 kHz	+19
22 mV	2.5 kHz	0
	5 kHz	+2
	10 kHz	+3
	20 kHz	+19

In figure 2, inductances L_0, L_2 and capacitance C_3 are located on the chip, the resistance R_2 and a part of the capacitance C_2 represent the twisted pair leads in the cryogenic probe and C_2–L_1–R_3–C_1 are the added physical components of the filter. The cable represents the coaxial connection to the thermal converter, and R_1–C_4 are the input impedances of the transfer standard.

The filter capacitance produces large, frequency-dependent ac–dc differences, the magnitude of which increases with capacitance and frequency. Simulations of the output transmission line indicate that the ac–dc difference contribution of the transmission line to the overall ac–dc difference in the ACJVS at frequencies above about 10 kHz depends critically on the value of the resistor, R_3, located between the cryoprobe head and the low-pass filter, which matches the output impedance of the cryoprobe section of the transmission line to the nominal filter source impedance. The corrections required due to the transmission line are shown in table 1. At present we do not have sufficient knowledge of the characteristics of the on-chip section of the transmission line to predict the value of R_3 required to make the contribution of the transmission line negligible; instead, we measure the transfer standard at 100 kHz and adjust R_3 (60 Ω for the measurements presented here) so that the measured ac–dc difference is independent of the frequency from 10 kHz to 100 kHz. As this is an insufficient determination of the transmission line characteristics, for the purposes of this paper we restrict the upper frequency of the measurements to 10 kHz, where both simulation and measurement indicate that the contribution of the transmission line is negligible.

4. Measurements and results

4.1. Ac–dc difference measurements

A key advantage of using a chip with two independently biased Josephson arrays (identified as left and right) is the number of possible measurements that can be made with each array in order to provide added confidence and redundancy in the measurements. In addition to traditional ac–dc measurements, we can also compare the ac performance of the system by using the TTS to compare the ac voltage supplied by each array. We can also use each array separately to measure the transfer standard at the same voltage (100 mV per array, for example) and compare the results with measurements made with both arrays in series (50 mV per array). For a perfect quantum system, we expect the mismatch between the two arrays to be negligible to within the repeatability of the TTS and the digital voltmeter used to measure the output of the transfer standard, both of which we expect to be quite good from measurement to measurement [10]. Note that for these measurements we require only that the transfer standard be stable, and not that the ac–dc difference be small.

To provide added confidence in our measurements, we calibrated the TTS with four ac Josephson chips of different designs (serial numbers 25, 32, 18I and 20B), mounted one at a time in the same cryoprobe, but with different connections between arrays and from the arrays to the output connector of the cryoprobe. As with the intra-array differences, we expect to see negligible variation in performance using several different chips.

The commercial TTS was measured at voltages between 2 mV and 200 mV, at frequencies from 2.5 kHz to 100 kHz, although in this paper we report results only for 10 kHz. These measurements encompassed the two lowest voltage ranges (22 mV and 220 mV) on this instrument. Multiple sets of measurement points were taken for each applied voltage and frequency for ac–dc transfer measurements. The typical measurement sequence (ac, dc+, ac, dc−) was completed in less than 20 min, so the drifts of the system electronics, TTS and the transfer function of the transmission line over the measurement interval were negligible.

Figure 3 presents the ac–dc differences obtained by using the ACJVS to calibrate the transfer standard, at an applied voltage of 10 mV on the 22 mV range of the transfer standard. The results are from the measurements using three different Josephson chips and include the average ac–dc difference for each array (or both arrays in series), the average ac–dc difference for all points on each frequency and the assigned uncertainty from table 5 in section 5. The correction for the transmission line listed in table 1 is not included. Figures 4 and 5 present similar data for 20 mV applied to the 22 mV range and for 100 mV applied to the 220 mV range. It should be noted that when the arrays are used in series with each array supplying one-half the total voltage, the ACJVS is programmed using a different digital code for the arrays than when one individual array supplies the total voltage.

Table 2 presents the departure from the average ac–dc difference for each chip, taking the average of the data in figures 3–5, for left, right and both arrays.

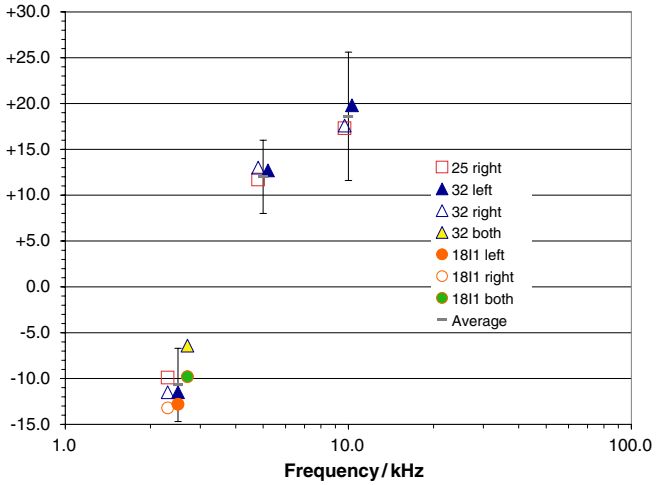

Figure 3. The ac–dc difference of the transfer standard with 10 mV applied to its 22 mV range. The error bars represent the uncertainties given in table 5 in section 5.

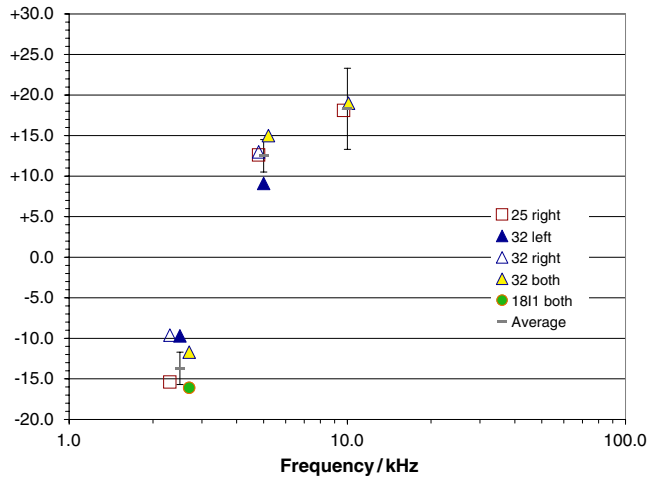

Figure 4. The ac–dc difference of the transfer standard with 20 mV applied to its 22 mV range. The error bars represent the uncertainties given in table 5 in section 5.

Table 2. Departure of each chip from the average ac–dc difference at each voltage listed in tables 2–4.

Voltage range/ mV	Applied voltage/ mV	Josephson chip	Departure from average ac–dc difference/μV V^{-1}		
			2.5 kHz	5 kHz	10 kHz
22	10	25	+0.8	−0.3	−1.3
		32	+0.2	+0.8	+0.8
		18I1	−1.7		
22	20	25	−1.7	+0.2	−0.2
		32	+3.3	−0.4	+0.7
		18I1	−2.5		
220	100	18I1	−1.4		
		20B	+1.1		

The 200 mV output of chip 20B allows us to make a direct comparison of our multijunction thermal converters [4] against the ACJVS. The results of the triangle between the TTS, MJTC and ACJVS at 2.5 kHz are shown in figure 6. The closure of the triangle (ACJVS + MJTC − TTS) is about −2 μV V^{-1}.

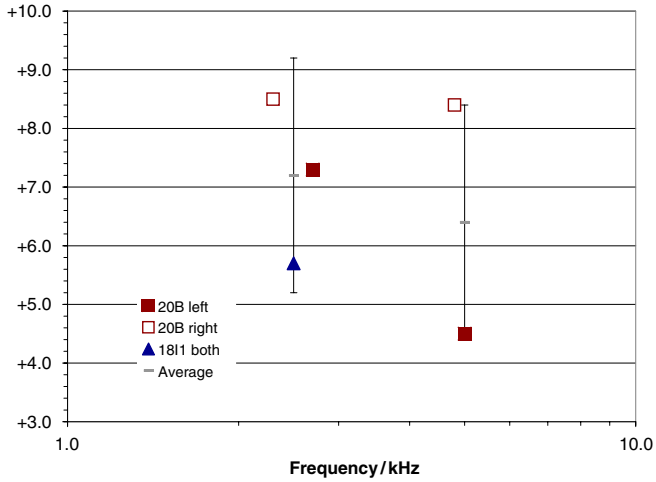

Figure 5. The ac–dc difference of the transfer standard with 100 mV applied to its 220 mV range. The error bars represent the uncertainties given in table 5 in section 5.

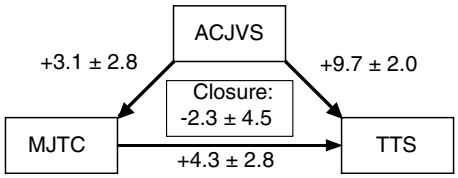

Figure 6. Result of intercomparisons between the ACJVS, TTS and MJTC in μV V^{-1}.

It should be noted that, even though the MJTC has a large dynamic range, the output voltage at 200 mV applied was less than 1 mV. The difficulty in measuring this small output voltage is the dominant contribution to the failure of the triangle to close.

4.2. Intra-array ac–ac measurements

Although we use both polarities of dc to measure the transfer standard, the ac–dc measurements described above may be subject to errors from thermal emfs when dc voltage is supplied by the ACJVS. We can determine the magnitude of the influence of these thermal effects by measuring the two on-chip arrays against each other at the same frequency of ac voltage. If no other errors are present, the two arrays should agree to within the short-term stability of the transfer standard.

Table 3 presents the results of such intra-array tests for two chips. The minute intra-array differences indicate that thermal emfs do not contribute significantly to the ac–dc differences shown in tables 2–4 and also strengthen our assumption that the ACJVS chip is a true intrinsic standard.

A fabrication flaw in chip 20B resulted in the left array having two shorted Josephson junctions (5118 working junctions as compared with 5120 for the right array). This flaw presents the opportunity to compare the measured difference in the two arrays with the difference predicted by the variation in the number of junctions. We would expect the output of the left array to be (5118/5120) or 390.6 μV smaller than the right array. In fact, we measure a difference of 387.8 μV with a standard deviation of 2.7 μV.

Table 3. Results of intra-array ac–ac comparisons in μV V^{-1}. The input voltage is 10 mV on the 22 mV range of the transfer standard. σ_{pooled} is the pooled standard deviation of multiple measurements.

	2.5 kHz		5 kHz		10 kHz	
Chip	δ	σ_{pooled}	δ	σ_{pooled}	δ	σ_{pooled}
32	0.0	0.2	0.0	0.1	+0.1	0.1
18I1	0.0	0.2	−0.2	0.2	−0.5	0.3

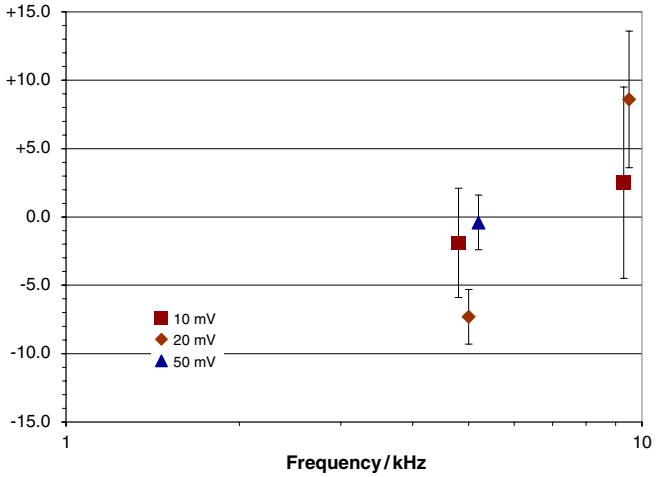

Figure 7. Comparison of the ac–dc difference predicted from ac–ac measurements with direct ac–dc measurements. The uncertainty bars are the uncertainties given in table 5 in section 5.

4.3. Synchronized ac–ac measurements

To remove the thermal effects present with dc voltage and to increase the speed of the measurements, we can measure the ac–ac differences at various frequencies relative to 2.5 kHz and reference them to dc by performing an ac–dc difference measurement at 2.5 kHz. To accomplish this, we use a synchronization circuit to synchronize the phases of the arbitrary waveform generators to the digital waveform at the measurement frequency and at 2.5 kHz and switch between waveforms. Making synchronized ac–ac measurements is much more efficient than ac–dc measurements since there is no need to tune the arrays for both polarities of dc voltage, and it increases the speed of data collection as well.

Figure 7 presents ac–ac data for several points and compares the ac–dc difference predicted from the ac–ac measurements with the actual measured ac–dc difference. The cause of the apparent frequency dependence of the disagreement in the (predicted − measured) values is unknown and presently under investigation.

5. Uncertainty analysis

Assuming that the ACJVS synthesized voltages are of quantum accuracy, the dominant contributions to the uncertainty for the system are Type A contributions of the measurement process, including the behaviour of the transfer standard and the characterization of the transmission line. Simulations of the transmission line model shown in figure 2 indicate that the uncertainty is critically dependent on the knowledge of

Table 4. Type B uncertainties associated with the circuit elements comprising the output transmission line, in $\mu V\,V^{-1}$.

Parameter	2.5 kHz	5 kHz	10 kHz
R_2	0.5	0.5	2.0
C_1	0.0	0.5	0.5
C_2	0.3	0.7	2.3
L_1	0.3	0.7	2.7
L_2	0.0	0.0	1.0
C_3	0.0	0.0	0.0
L_0	0.0	0.0	0.0
Cable length	0.5	0.5	2.0
Expanded uncertainty ($k = 2$)	0.7	1.5	4.9

Table 5. Expanded uncertainties provided in first calibration of a TTS against the quantum ac source.

Voltage range/	Applied voltage/	Uncertainty/($\mu V\,V^{-1}$ of applied voltage)		
mV	mV	2.5 kHz	5 kHz	10 kHz
22	6	12	11	12
22	10	4	4	7
22	20	2	2	5
220	60	1	4	6
220	100	2	2	5

the total resistance of the transmission line between the probe head and the transfer standard. To determine the effect on the ac–dc difference caused by small changes in the values of the circuit elements in figure 2, the values of these circuit elements were altered in the simulation and the changes to the predicted output voltage noted for different frequencies. Table 4 lists Type B uncertainties, calculated using $u_C^2(V) = \sum_{i=1}^{n} [\partial P/\partial x_i]^2 u^2(x_i)$ [11] associated with the circuit elements, as well as the final Type B uncertainty for the ACJVS.

Of course, the final expanded uncertainty for a calibration of the transfer standard also depends upon Type A components (which we have taken to be the pooled standard deviations of multiple measurements) of the measurement process. We have recently provided a calibration that includes the world's first measurements against a quantum ac standard. The expanded uncertainties provided for the points measured with the ACJVS are shown in table 5.

The uncertainties listed in table 5 represent a significant improvement over the uncertainties normally provided on this instrument based on a characterization using traditional step-down techniques. For 6 mV applied at 10 kHz, for example, the uncertainty presented in table 5 is more than an order of magnitude smaller than the routine NIST uncertainty for this voltage and frequency ($12\,\mu V\,V^{-1}$ was compared with $183\,\mu V\,V^{-1}$). The improvements in uncertainty are greatest at the lowest voltages where the uncertainties are larger because of range-to-range scaling. At higher voltages, some improvements in uncertainties are noted, but because the scaling is more accurate at these voltages, the reductions in uncertainty are not as dramatic. It is also worth noting that the values measured using the traditional range-to-range scaling procedure agree with the values obtained using the ACJVS to well within the uncertainty obtainable using the traditional techniques. This confirms that the scaling process from the 2 V level of the primary standards to the 2 mV range provides accurate calibrations of TTSs and that our uncertainties at these low voltages may be too conservative.

6. Future work

The most urgent task for the near future is to fully characterize the output transmission line. Currently, the only way we can characterize the transmission line containing the series resistor and filter is to minimize the frequency coefficient of the transfer standard from 2.5 kHz to 100 kHz, but this is unsatisfying from a metrological point of view and requires us to redetermine the frequency coefficient for each ACJVS chip. A full characterization of the transmission line out to 1 MHz is required to realize the performance of the quantum ac source to higher frequencies independent of the chip.

Currently, collection of data using the ACJVS is fully automated, but the bias conditions are set manually. At least eight manual adjustments are required to bring the arrays onto their operating margins for ac–dc difference tests. Ac–ac measurements require fewer adjustments, but are still labour intensive. The cost of manually operating the ACJVS system may prevent its inclusion into the routine calibration service for ac–dc difference. We plan to pursue automating the system as much as possible; however, full automation of the system requires improvements in the bias electronics. In the interim, we plan to characterize several of our TTSs against the ACJVS and use these instruments in the routine calibration system. The resulting uncertainties will not match those available in a direct comparison with the ACJVS but will be significantly better than the present routine uncertainties.

7. Conclusions

We have described the first quantum ac measurement system used for calibrating a customer's TTS. The uncertainties provided to this customer are, at the lowest voltage ranges, more than an order of magnitude smaller than uncertainties available using traditional scaling methods. We are currently calibrating several of our TTSs up to 200 mV to propagate the performance of the ACJVS to a cost-effective calibration service for TTSs. We plan to fully characterize the output transmission line in order to reduce the uncertainties of the ACJVS at frequencies of up to 1 MHz.

Acknowledgments

The authors would like to thank Norm Bergren and Regis Landim for their significant contributions to the development of the ACJVS.

References

[1] Hermach F L 1952 Thermal converters as ac–dc transfer standards for current and voltage measurements at audio frequencies *J. Res. Natl Bur. Stand. (US)* **48** 121–38
[2] Inglis B D 1992 Standards for ac–dc transfer *Metrologia* **29** 191–9

[3] Hermach F L, Kinard J R and Hastings J R 1987 Multijunction thermal converters as the NBS primary transfer standards for ac voltage and current measurements *IEEE Trans. Instrum. Meas.* **36** 300–6
[4] Kinard J R, Huang D X and Novotny D B 1995 Performance of multilayer thin-film multijunction thermal converters *IEEE Trans. Instrum. Meas.* **44** 383–6
[5] Kinard J R, Lipe T E, Tang T, Benz S P, Burroughs C J and Dresselhaus P D 2007 Calibration of thermal converters using a quantum AC source *Proc. 2007 NCSLI Workshop Symp. (St Paul, MN, 29 July–2 August 2007)* paper 1E-1 (CD)
[6] Benz S P and Hamilton C A 1996 A pulse-driven programmable Josephson voltage standard *Appl. Phys. Lett.* **68** 3171–3
[7] Burroughs C J, Benz S P, Dresselhaus P D and Ching Y 2005 Precision measurements of AC Josephson voltage standard operating margins *IEEE Trans. Instrum. Meas.* **54** 624–7
[8] Benz S P, Burroughs C J, Dresselhaus P D, Bergren N F, Lipe T E, Kinard J R and Tang Y 2007 An AC Josephson voltage standard for AC–DC transfer-standard measurements *IEEE Trans. Instrum. Meas.* **56** 239–43
[9] Kieler O F, Landim R P, Benz S P, Dresselhaus P D and Burroughs C J 2007 AC–DC transfer standard measurements and generalized compensation with the AC Josephson voltage standard *Proc. 2007 NCSLI Workshop Symp. (St Paul, MN, 29 July–2 August 2007)* paper 1E-3 (CD)
[10] Landim R P, Benz S P, Dresselhaus P D and Burroughs C J 2008 Systematic-error signals in the ac Josephson voltage standard: measurement and reduction *IEEE Trans. Instrum. Meas.* at press
[11] Taylor B N and Kuyatt C E 1993 Guidelines for evaluating and expressing the uncertainty of NIST measurement results *Natl Inst. Stand. Technol. Tech. Note* 1297